Journal of Agrometeorology
(A publication of Association of Agrometeorologists)
ISSN : 0972-1665 (print), 2583-2980 (online)
Vol. No. 28 (2) : 221-229 (June - 2026)
https://doi.org/10.54386/jam.v28i2.3336
https://journal.agrimetassociation.org/index.php/jam

Research paper

Future Precipitation Dynamics and Their Implications for Agricultural Water Security in Iraq: A PlaSim Assessment

DOHA A. SOROR and MUTHANNA A. AL-TAMEEMI*

Department of Atmospheric Science, College of Science, Mustansiriyah University, Baghdad, Iraq

ABSTRACT

Rainfall changes across Iraq were explored under two Shared Socioeconomic Pathways (SSPs): SSP1–2.6 (low-emission) and SSP2-4.5 (medium-emission) using the Planet Simulator (PlaSim) model. Bias correction of precipitation dynamics was performed against ERA5 reanalysis data (1995–2024) for near-future (2026–2050), mid future (2051–2075), and far future (2076–2100) scenarios. Under SSP1-2.6, precipitation shows a U-shaped trajectory with a 24% decrease (near-future) and gradual recovery to 9% below baseline by 2100 along with increased interannual variability. Under SSP2-4.5, significant deficits of 16–21% endure through each interval with negligible variation. These divergent trajectories have significant consequences for rainfed winter wheat production in northern Iraq, which relies on winter-spring precipitation (DJF-MAM). SSP1-2.6 Increased variability under threatens the predictability of crop phenology, while SSP2-4.5 Fundamental reshaping of these agricultural systems would be essential to avoid chronic deficits in food availability. The differences highlight the extent to which global emission pathways will seal Iraq's fate when it comes to water security and agricultural viability.

Keywords: Climate change, Iraq, Precipitation, PlaSim, SSP scenarios, Water resources

Global surface temperatures are projected to increase beyond mid-century for all emissions scenarios, fundamentally changing the hydrological cycle and causing massive alterations in precipitation with serious consequences for water resources, food security and ecosystems globally (Arias *et al.,* 2021) (Lee *et al.,* 2023). These changes are already affecting arid and semi-arid regions including the Middle East and North Africa (MENA), leading to worsening vulnerability. (Al-Addous *et al.,* 2024).

To forecast these impacts, scientists rely on Global Climate Models (GCMs), the most recent generation of which is that provided by Coupled Model Intercomparison Project Phase 6 (CMIP6). But those models come with their own pitfalls. In summary, a recent study evaluated 16 different CMIP6 models and showed both systematic errors and biases in the precipitation simulated by these models, especially regions with complex orographic systems and found that most of the models have a dry bias. This highlights the need for careful model selection and bias correction in future regional scale assessments of climate impacts (Tiku *et al.,* 2025).

In the heart of MENA, Iraq has a hot to semi-arid climate and is heavily dependent on the Tigris and Euphrates rivers. The country is already feeling the effects of the climate crisis, with more frequent droughts, heatwaves and dust storms contributing to declining precipitation and rising temperatures that aggravate its water emergency (Al-Daoudi & Al-Timimi, 2024) (Aleedani *et al.,* 2024). Next to the local climate factors, the global character of climate determines Iraq through global oscillations. Recent studies have indicated a potential linkage of Pacific climate variables to Iraq through teleconnections involving the El Niño Southern Oscillation (ENSO) (Al-Tameemi *et al.,* 2025). But the wider consequences of these changes are dire for Iraq's agriculture, which is the backbone of the rural economy**.** Winter staple crops (wheat and barley), sown in October-November, depend critically on precipitation during winter (DJF) and spring (MAM) months. Any significant alteration to these seasonal rainfall patterns threatens rainfed agriculture in the north and stresses irrigated systems in central and southern regions that depend on river discharge sourced from the same seasonal precipitation.

Nevertheless, recent research has to clarified the

Article info - DOI: *https://doi.org/10.54386/jam.v28i2.3336*
Received:09 January 2026; Accepted: 11 April 2026; Published online : 04 June 2026

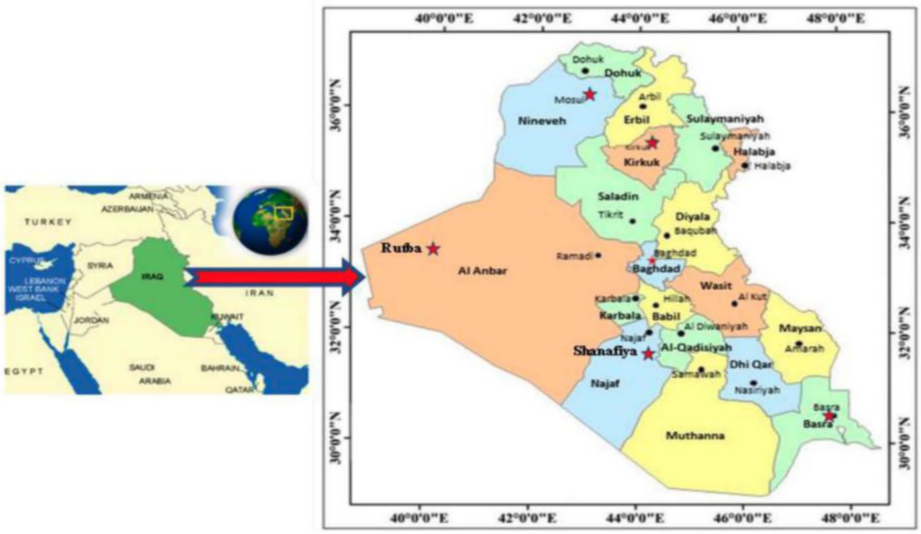

Fig. 1: Study area (Iraq map; Khaleel *et al.,* 2025)

complexity and often contradictory nature, of climate projections for the MENA. Rainfall predictions for 1.5°C and 2.0°C warming scenarios indicate a notable rise (up to 50%) for several nations, including Iraq, changing some regions from hyper-aridity to aridity (Hamed *et al.,* 2024). However, a multi-model CMIP6 ensemble analyzed by (Francis & Fonseca, 2024) projects subtropical highs in some regions to move poleward and the tropical easterly jet to weaken, consistent with drying in portions of the region. With regard to Iraq, (Hashim *et al.,* 2024) used statistical downscaling of CMIP6 data to predict that although a few rainy years are likely in the near and mid-future, the southwestern part of Iraq will remain under a state of severe drought and precipitation shortage. These contrasting findings highlight the large uncertainty in regional climate Change projections.

The present study uses the Planet Simulator model (PlaSim), a General circulation model of intermediate complexity (hereafter: GCM-IC), developed by the University of Hamburg (Angeloni *et al.,* 2020), and seek to specifically contribute to a better understanding of future rainfall changes in Iraq. PlaSim is an intuitive climate modelling tool that simulates the global climate system, including the hydrological cycle, through its land, precipitation, evaporation and surface heat flux component. Using PlaSim under two different Shared Socioeconomic Pathways (SSPs): SSP1-2.6 (low emissions) and SSP2-4.5 (medium emissions) we provide a detailed account of projected rainfall changes over Iraq, on near-future (2026-2050), mid-future (2051-2075) and far-future (2076-2100) time intervals. These results can help identify sections of agricultural policies in Iraq that need to embrace climate adaptation changes to mitigate potential damage by water scarcity outcomes.

MATERIALS AND METHODS

In this stydy we used the Planet Simulator (PlaSim), a General Circulation Model (GCM) of intermediate complexity, which was developed at the Meteorologisches Institut, Universität Hamburg (Fraedrich *et al.,* 2005). PlaSim was set up at a horizontal resolution of T42 (128 × 64 grid boxes) using 10 non-equidistant vertical levels in sigma-coordinates and with a time step of 45 min. Although the PlaSim T42 resolution is relatively coarse for local-scale impact assessments, this limitation is mitigated by applying the Multiplicative Bias Correction (MBC) method, which improves the reliability of the simulations for country-level climate analysis.Two scenarios were considered for projecting future precipitation: SSP1-2.6 (Low Emission, consistent with Paris Agreement 1.5°C target) and SSP2–4.5 (Medium emission approx 2.4degree warming by 2100) (Arias *et al.,* 2021). The simulations are provided for three time periods, which are Near-Future (2026–2050), Mid-Future (2051–2075), and Far-Future (2076–2100).

To validate the models, the ERA5 reanalysis dataset from Copernicus Climate Change Service (C3S) was used (Store, 2023). For the validation period 1995-2024, daily total precipitation data are available at 0.25° × 0.25° spatial resolution (~28 km) from ERA5. Daily precipitation values of both ERA5 and PlaSim were extracted for the whole Iraq domain (28°N to 38°N, 38°E to 50°E) and then spatially averaged into country daily value. A Multiplicative Bias Correction (MBC) method (also linear scaling) which applies a scaling correction where the correction factor is the mean observed annual precipitation divided by the mean model annual precipitation ratio was used to correct systematic model biases. Then this correction factor was consistently applied to all daily precipitation values as P_corrected(t) = P_model(t) × CF. This method retains the temporal ordering and interannual variability of model precipitation, but is consistent with non-negativity constraints, and again, appropriate for the multiplicative bias structure of precipitation (Dhawan *et al.,* 2024). The daily precipitation data were subsequently averaged to a monthly and an annual scale after the correction for the analysis of future rainfall changes in Iraq. Iraq is situated in the south-western part of Asia, between 29.6°N and 37.5°N latitudes and 38.45°E and 48.45°E longitudes as shown in (Fig.1). Iraq's topography consists of diverse physiographic regions, including a mountainous region in the north, an alluvial plain in the central and in the south and west. Annual precipitation of around 1,000 mm in the northern mountains compared to less than 100 mm in the southern deserts. This hydroclimatic divide dictates the country's agrometeorological landscape: the northern governorates, such as Dohuk, Erbil, and Sulaymaniyah, largely practice rainfed agriculture, while the central and southern regions are almost entirely dependent on irrigation from the Tigris and Euphrates rivers for agricultural production. (Wahab *et al.,* 2023).

RESULTS AND DISCUSSION

In this study, future precipitation changes in Iraq are compared under two different Shared Socioeconomic Pathways (SSPs): the low-emission SSP1-2.6 and the medium-emission SSP2-4.5. The future rainfall distribution and trend under the two scenarios are summarized in Table 1. This yields two dramatically different futures while the hydroclimate of the country is highly sensitive to the global emission pathway. This analysis also offers important insights for national adaptation planning and underscores the necessity of flexible strategies that will be effective across diverse climate futures.

Temporal Evolution of Annual Precipitation: Comparative Analysis of SSP1-2.6 and SSP2-4.5

The temporal pattern of annual precipitation shows two fundamentally different hydroclimatic futures for Iraq, based on the global emission pathway. Under the low-emission SSP1-2.6 Scenario (Fig. 2), statistically significant positive trend of +0.83 mm/year suggests gradually, albeit somewhat lagged recovery. The 5-year running mean (Fig. 2a) at the other end of the spectrum, showing a clear upward trend after 2050, nearly reaching the historical baseline (256 mm) by century's end. However, the cumulative anomaly (Fig. 2d) with a roughly -3,000 mm balance, indicating a significant and continuous water deficit over the 75-year simulation period. (Fig. 2b) shows the 12-month moving average of monthly rainfall, highlighting seasonal fluctuations and a gradual upward trend towards recovery at the end of the century under the SSP1-2.6 scenario. The annual anomalies (Fig. 2c) remain largely negative but with more frequent and larger magnitude positive excursions in the far-future, indicating enhanced interannual variability rather than a systematic change to a wetter-than-baseline climate. In stark contrast, the SSP2-4.5 scenario (Fig. 3) predicts climatic stagnation. Fig. 3a shows the trend is negligible (+0.15 mm/year), and the 5-year running mean remains flat, oscillating around 200 mm, approximately 20% below the historical baseline. The 12-month moving average in (Fig. 3b) clearly shows the long-term upward trend in rainfall, confirming a gradual recovery path towards historical baseline levels by the end of the century. This persistent deficit results in a more severe cumulative water loss, reaching approximately -3,800 mm by 2100 (Fig. 3d). The annual anomalies (Fig. 3c) are almost uniformly negative, indicating a chronic state of water stress with no recovery trajectory. The primary distinction is clear: SSP1-2.6 offers a path toward partial hydrological recovery driven by a positive trend, while SSP2-4.5 locks Iraq into a future of intensified and unceasing aridity.

The table1 reveals a gradual recovery in rainfall under the SSP1-2.6 scenario, with the deficit reaching 9.3% by the end of the century, compared to continued chronic drought under the SSP2-4.5 scenario, with a deficit exceeding 16%.

Distributional and Seasonal Characteristics

Under the SSP1-2.6 scenario, the precipitation distribution displays a distinct rightward shift and expands in interquartile range

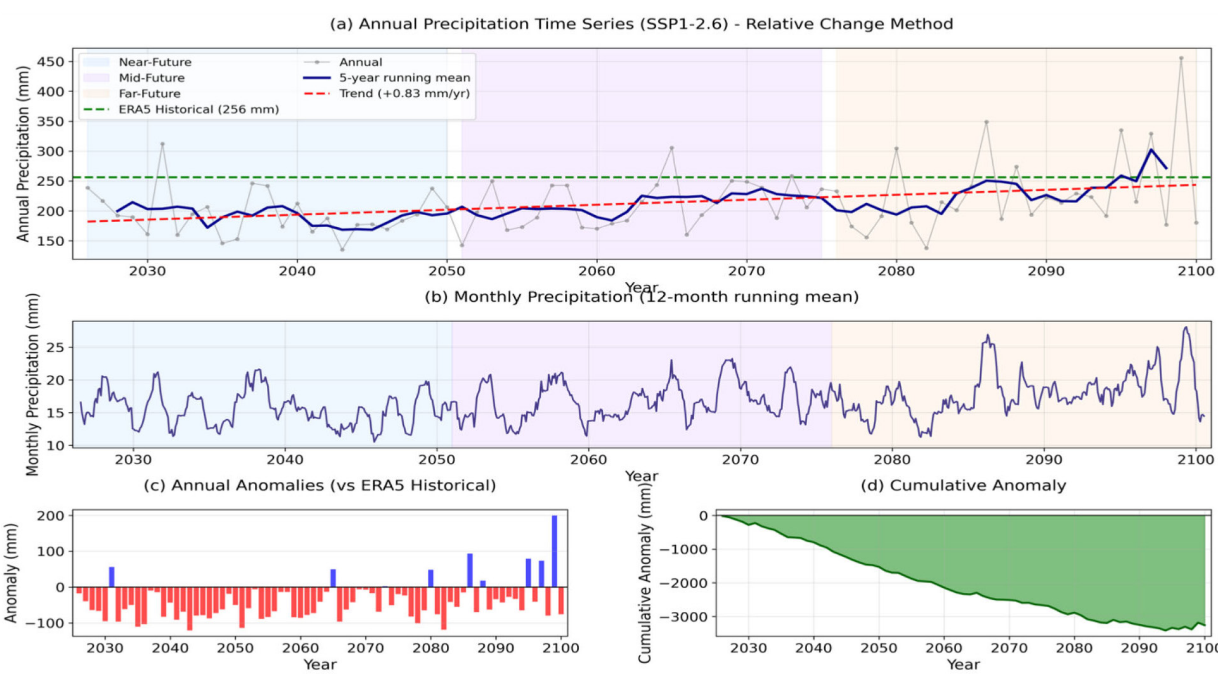

Fig. 2: Annual precipitation time series (SSP1-2.6): (a) annual values with trend, (b) 12-month running mean, (c) anomalies, (d) cumulative anomaly.

Table 1: Summary Statistics for Annual Precipitation (SSP1-2.6 and SSP2-4.5 Scenarios)

Period	SSP1-2.6			SSP2-4.5		
	Mean (mm/year)	Std Dev (mm)	Change vs Baseline (%)	Mean (mm/year)	Std Dev (mm)	Change vs Baseline (%)
Near-Future (2026-2050)	195.0	38.2	-23.9%	204.3	31.9	-20.2%
Mid-Future (2051-2075)	210.7	38.7	-17.7%	203.7	41.9	-20.5%
Far-Future (2076-2100)	232.3	71.2	-9.3%	212.7	25.7	-16.9%

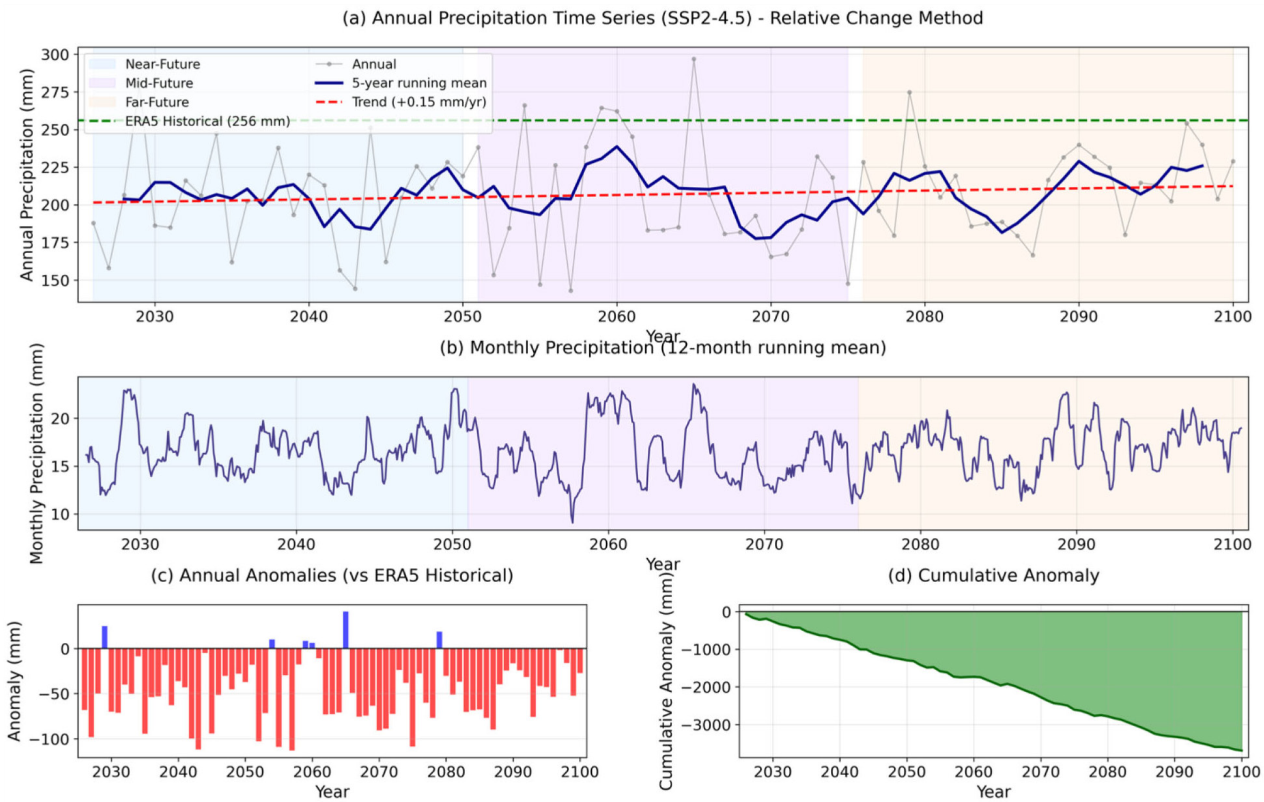

Fig. 3: Annual precipitation time series (SSP2-4.5): (a) annual values with trend, (b) 12-month running mean, (c) anomalies, (d) cumulative anomaly.

from 170–230 mm (Fig. 4a) up to 180–280 mm, suggesting increased hydroclimatic variability. This widening indicates increased availability of moisture in the atmosphere and thermodynamic amplification from increased warming, which is consistent with Clausius–Clapeyron relation scaling of precipitation extremes. And although widespread deficits remain entrenched well into the near-to-mid term future, that distributional shift higher in values does indicate greater odds of intense rain events. In aggregate, these alterations suggest a shift of the climate system to a new equilibrium state that will be more variable and have more extreme behavior.

The seasonal precipitation structure (Fig. 4b) shows a modest reorganization under SSP1-2.6, indicating a small decrease in DJF totals compared to the historical baseline and an evident increment of SON from ~20–25 mm to 30–40 mm. This transition implies a reallocation from a predominately winter-controlled system to increased autumn precipitation, possibly associated with alterations in the dynamics of the mid-latitude storm track and moisture fluxes between seasons. The monthly climatology (Fig. 4c) also supports this behaviour, as it exhibits a decrease of the winter peak alongside the establishment of an autumn maximum and modification of the seasonal cycle structure. Furthermore, the anomaly distribution (Fig. 4d) changes from mostly negative conditions during the near future (~−20% to −30%) to less negative values in the distant future (~−10%), indicating an increased relative frequency of near- to above-baseline precipitation years.

Projections under SSP2-4.5 reveal a continuing moisture deficit relative to the ERA5 historical normal (255 mm). The MAP shows little variation at around 205 mm for near and mid-future (Fig. 5a) with a slight recovery to 215 mm by far-future. A seasonal analysis (Fig. 5b) shows that DJF continues to be the most prominent rainy season (95–100 mm), whereas SON appears slightly more intense late-century with a minor increase to 30 mm.

Future precipitation stays well below historical values

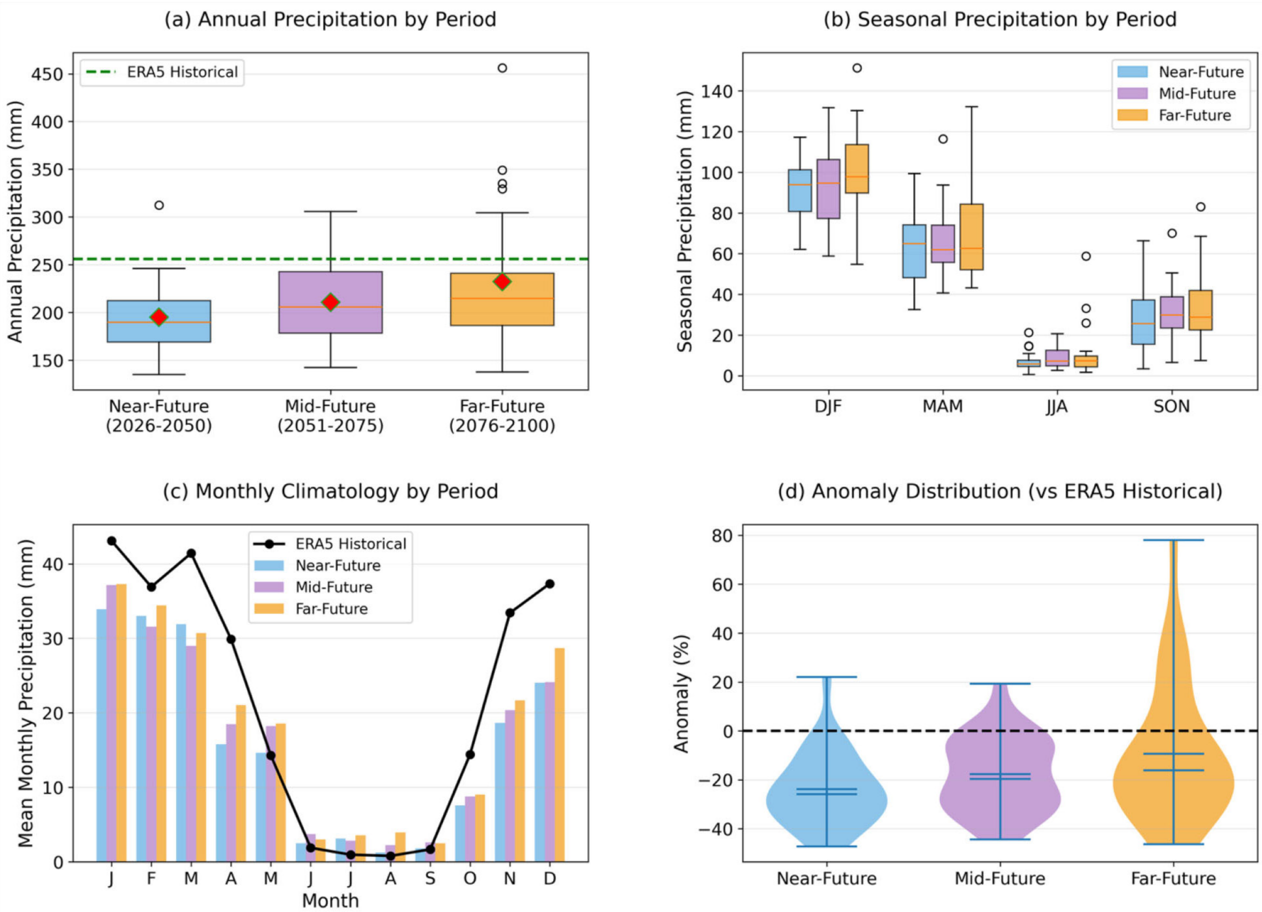

Fig. 4: Distributional analysis (SSP1-2.6): (a) annual precipitation by period, (b) seasonal precipitation, (c) monthly climatology, (d) anomaly distribution.

across most months in monthly climatology (Fig. 5c), especially for core winter months. This is also evident in the anomaly distribution (Fig. 5d), with median anomalies remaining at -20% to -17%. Unlike previous high-variability projections, the far-future distribution is bimodal with much reduced variance and cannot predict extreme positive anomalies exceeding +10%. These results indicate that the future is more likely to be characterized by chronic aridity than hydrologic recovery, and adaptation to a permanent lower-precipitation regime will be needed over the long term.

Seasonal Precipitation Trends: Differential Forcing Sensitivity

Under SSP1-2. As shown in Fig. 6a (top-left), over DJF, a positive trend of +0.20 mm/year is evident, with the 5-year running mean increasing from 90 mm to 105 mm (and indeed winter precipitation intensification continues). The MAM (Fig. 6b, top-right) exhibits a very weak trend (+0.15 mm/year) with values remaining around 70 mm, consistent with spring precipitation's insensitivity to anthropogenic warming. The JJA season (Fig. 6c, lower left) shows almost no trend (+0.09 mm/year) with the moving average close to 10 mm, indicating persistent summer dryness. SON season (Fig. 6d, bottom-right) show the most rapid response with trend +0.13 mm/year and running mean accelerating from 25 mm to 40 mm together +60% to become a prominent rainfall period in autumn.

Under SSP2-4.5 In DJF season though (Fig. 7a), the trend is weak (+0.08 mm/year) and running mean stays around 95 mm, consistent with climatic persistence. In contrast, the MAM season (Fig. 7b) shows no trend (+0.04 mm/year) and is centered around 70 mm, with no systematic change. In the JJA season (Fig. 7c), trend is near-zero (+0.03 mm/year), retaining ~8 mm. SON season (Fig. 7d) is showing near stable value (25 mm) characterized by a low magnitude of negative trend (-0.03 mm/year).

The mechanistic divergence is stark: SSP1-2.6's favorable DJF and SON changes suggest reorganization of circulation, which both recuperates wintertime intensity and strengthens autumnal grow seasons, while also contrasting with SSP2-4. 5's weak or negative trends suggest that competing mechanisms (moisture intensification versus subtropical high-pressure expansion) inhibit reshaping through the seasons. This trend difference has a direct effect on water availability: SSP1-2.6 initiates a bimodal (winter-autumn) precipitation regime, whereas SSP2-4.5 keeps a winter over inflated regime going with continued spring-summer shortages.

Although summer (JJA) precipitation is limited over central and southern Iraq in both scenarios, increases projected for high elevation precipitation over northern uplands regions (outside of the core study domain) have major importance for downstream water availability. Summer precipitation falling on the Zagros

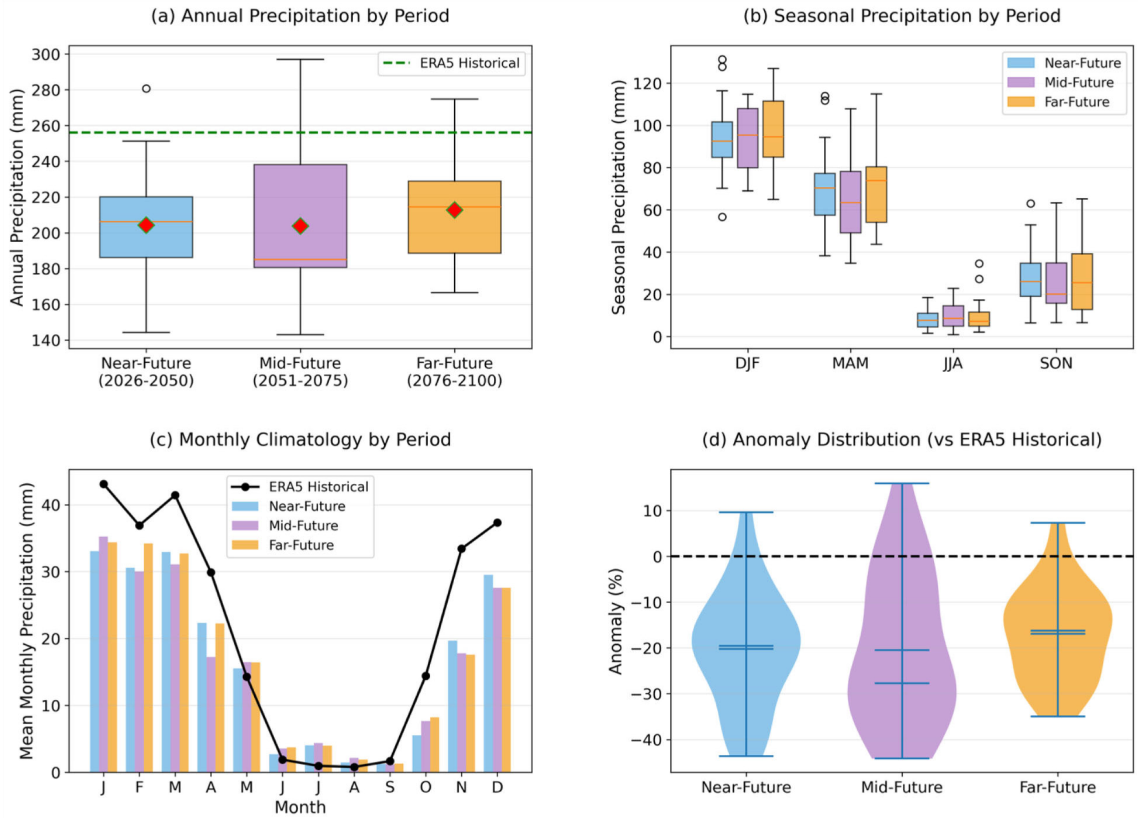

Fig. 5: Distributional analysis (SSP2-4.5): (a) annual precipitation, (b) seasonal, (c) monthly climatology, (d) anomaly distribution.

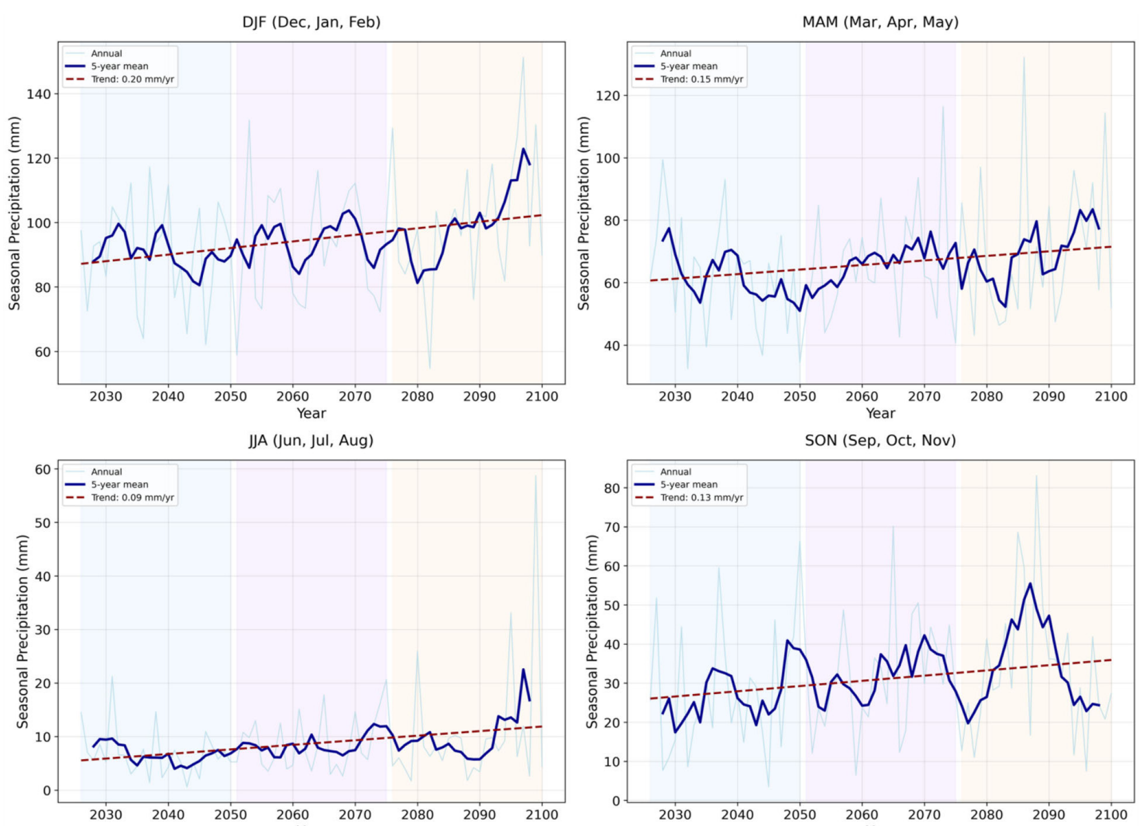

Fig. 6: Seasonal precipitation trends (SSP1-2.6): DJF, MAM, JJA, and SON.

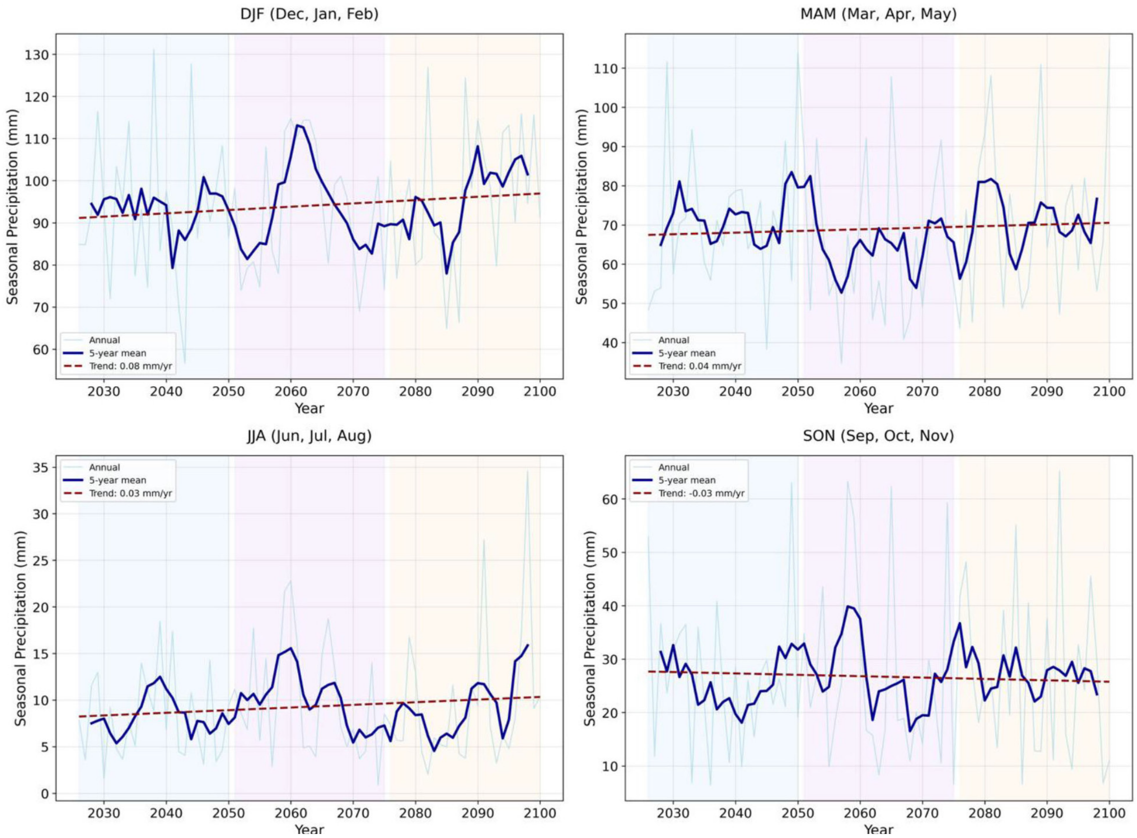

Fig. 7: Seasonal precipitation trends (SSP2-4.5): DJF, MAM, JJA, and SON.

Table 2: Comparative Summary of SSP1-2.6 and SSP2-4.5 Scenarios

Characteristic	SSP1-2.6	SSP2-4.5
Long-Term Trend	+0.83 mm/year (p=0.003)	+0.15 mm/year (p=0.426)
Trajectory	U-shaped recovery	Stabilized drying
Near-Future Change	-23.9% (-61 mm)	-20.2% (-52 mm)
Mid-Future Change	-17.7% (-45 mm)	-20.5% (-52 mm)
Far-Future Change	-9.3% (-24 mm)	-16.9% (-43 mm)
Cumulative Deficit	~-3,000 mm	~-4000 mm
Variability Trend	Increasing	Stable/Declining
Spatial Signal	Strong (mountains)	Weak (localized)

Mountains generates enhanced river runoff in the most critical growing season, acting as irrigation for summer crops in the central alluvial plains and southern areas. Under SSP1-2.6, increased summer precipitation in the mountains may increase dry season river discharge also, somewhat mitigating the chronic water stress faced by irrigation-dependent agricultural regions. Conversely, SSP2-4.5 The stagnation of high elevation precipitation would reinforce low summer river flows, intensifying water scarcity for irrigated agriculture.

Comparative Analysis between SSP1-2.6 and SSP2-4.5 Scenarios

The divergence between precipitation projections illustrates the vital role of global emission pathways for water security and agricultural stability in Iraq. SSP1-2. 6 projects large initial deficits (-23.9%) that gradually recover towards baseline (-9.3% by far-future) with increasing interannual variability SSP2-4. 5 projects have persistent deficits (-17% to -21%) with stable or declining variability, indicating that of a locked-in arid state As shown in Table 2.

Agrometeorological Implications: The different variability patterns have important implications for rainfed agriculture. Under SSP1-2.6, the rising interannual variability (Table 2) leads to uncertain precipitation regimes hampering crop phenomenology and optimization of plant date, which might increase risks of fail in dry years in spite of long-term recovery. Farmers would need adaptive management practices such as flexible planting windows, cultivars that resist drought and supplementary irrigation capacity to mitigate greater fluctuations from year to year. Conversely, SSP2-4.5's enduring shortfalls in stable variability pose a separate challenge: the chronic but predictable water stress calls for a fundamental course correction for agriculture, especially in rainfed northern domains. SP2-4.5, the cumulative deficit of

4,000 mm over 75 years 5 (compared to 3,000 mm under SSP1-2.6) show that in central and southern Iraq rainfed agriculture is becoming increasingly unviable. Widespread transition to irrigated agriculture will be necessary, dependent on management of river discharge and groundwater resources. Under SSP1-2.6, much of the recovery trajectory through the end of century will provide a route for more viable rainfed agriculture by century's end; however, this interim period (2026–2075) is one in which intense adaptation efforts are necessary. Under SSP2-4.5 adaptation has to centre on the development of irrigation infrastructure and water conservation technologies to ensure agricultural production persists under a context of ongoing water scarcity.

Uncertainty Quantification

Under SSP1-2.6, uncertainty progressively increases across periods: near-future (19.7%, 95% range: 141-273 mm/year), mid-future (18.3%, 95% range: 153-277 mm/year), and far-future (27.7%, 95% range: 148-392 mm/year), indicating a transition toward greater variability. The non-normal distribution (Shapiro-Wilk p=0.0022) justifies the empirical percentile approach. In contrast, SSP2-4.5 exhibits more stable uncertainty across periods: near-future (16.6%, 95% range: 152-263 mm/year), mid-future (20.7%, 95% range: 145-278 mm/year), and far-future (11.4%, 95% range: 174-262 mm/year), reflecting a predictable but persistently arid regime. Divergent patterns like these require different approaches: SSP1–2.6 demand adaptive infrastructure in response to greater variability, and SSP2-4.5, which needs resilience for continued water stress with ~20% baseline reduction. We should use 68% confidence intervals for operational planning while infrastructure design needs to be designed for 95% ranges to avoid extremes.

CONCLUSION

This study systematically quantifies anticipated precipitation throughout Iraq under SSP1–2. 6 and SSP2-4. 5 emission scenarios using PlaSim. Iraq's hydroclimate responds highly to global emission pathways. Under SSP1-2.6, the projected partial precipitation recovery by 2100 is offset by elevated interannual variability and reduces growing conditions for winter wheat in unpredictable ways. Under SSP2-4. 5, chronic water stress due to persistent precipitation deficits (16–21%) over the century is widespread. These contrasting futures have significant implications for agricultural and water security in Iraq. We suggest two agrometeorological adaptation strategies, (1) under SSP1-2. 6, adopt early maturing wheat varieties to escape end-of-season drought and take advantage of projected increases in autumn precipitation (SON) for supplementary irrigation; (2) under SSP2-4.5, shift to more drought-tolerant crop varieties and adopt deficit irrigation strategies that maximize water-use efficiency. Both these pathways require integration of seasonal climate forecasts into national water-management planning and coordinated regional adaptation measures.

ACKNOWLEDGEMENT

We acknowledge the Copernicus Climate Change Service (C3S) for providing ERA5 reanalysis data and the University of Hamburg for the Planet Simulator (PlaSim) model used in this study.

Author's certificate: The manuscript or its part is not under consideration for publication elsewhere and the same has been approved by all co-authors.

Conflict of Interests: The authors declare that there is no conflict of interest regarding the publication of this article.

Funding: No funding was received during the preparation of the manuscript.

Authors Contribution: **D. A. Soror**: Data collection, Data Analysis, Conceptualization, Methodology, Visualization, Writing original draft, Writing-review; **M. A. Al-Tameemi:** Supervision, Review, and editing.

Data availability statement: The data used in this study are available from the corresponding author upon reasonable request.

Disclaimer: The contents, opinions, and views expressed in the research article published in the Journal of Agrometeorology are the views of the authors and do not necessarily reflect the views of the organizations they belong to.

Publisher's Note: The periodical remains neutral with regard to jurisdictional claims in published maps and institutional affiliations.

REFERENCES

Al-Addous, M., Bdour, M., Rabaiah, S., Boubakri, A., Schweimanns, N., Barbana, N., & Wellmann, J. (2024). Innovations in solar-powered desalination: a comprehensive review of sustainable solutions for water scarcity in the Middle East and North Africa (MENA) region. *Water*, *16*(13), 1877.

Al-Daoudi, A. S., & Al-Timimi, Y. (2024). The Spatial Pattern Assessment of Annual Rainfall in Iraq for Periods from 2001 to 2023. IOP Conference Series: Earth and Environmental Science,

Al-Tameemi, M. A., Al-Nassar, A. R., Mutar, A. G., & Castrillon, A. (2025). The Telecommunications between Iraq Region Air Temperature and ENSO El NIÑO 3.4 Region. *Al-Mustansiriyah Journal of Science*, *36*(1), 1–13.

Aleedani, F. Y., Albattat, M. Q., & Badr, J. M. (2024). Rainfall Repercussions: Assessing Climate Change Influence on Iraq Precipitation Patterns. *Al-Kitab Journal for Pure Sciences*, *8*(01), 92–103.

Angeloni, M., Palazzi, E., & Von Hardenberg, J. (2020). Evaluation and climate sensitivity of the PlaSim v. 17 Earth System Model coupled with ocean model components of different complexity. *Geoscientific Model Development Discussions*, *2020*, 1–23.

Arias, P., Bellouin, N., Coppola, E., Jones, R., Krinner, G., Marotzke, J., Naik, V., Palmer, M., Plattner, G.-K., & Rogelj, J. (2021). Climate Change 2021: the physical science basis. Contribution of Working Group I to the Sixth Assessment Report of the Intergovernmental Panel on Climate Change; technical summary.

Dhawan, P., Dalla Torre, D., Niazkar, M., Kaffas, K., Larcher, M., Righetti, M., & Menapace, A. (2024). A comprehensive comparison of bias correction methods in climate model simulations: Application on ERA5-Land across different temporal resolutions. *Heliyon*, *10*(23).

Fraedrich, K. F., Jansen, H., Kirk, E., Luksch, U., & Lunkeit, F. (2005). The Planet Simulator: Towards a user friendly model. *Meteorologische Zeitschrift*, *14*(3), 299–304.

Francis, D., & Fonseca, R. (2024). Recent and projected changes in climate patterns in the Middle East and North Africa (MENA) region. *Scientific Reports*, *14*(1), 10279.

Hamed, M. M., Sobh, M. T., Ali, Z., Nashwan, M. S., & Shahid, S. (2024). Aridity shifts in the MENA region under the Paris Agreement climate change scenarios. *Global and Planetary Change*, *238*, 104483.

Hashim, B. M., Alnaemi, A. N. A., Hussain, B. A., Abduljabbar, S. A., Doost, Z. H., & Yaseen, Z. M. (2024). Statistical downscaling of future temperature and precipitation projections in Iraq under climate change scenarios. *Physics and Chemistry of the Earth, Parts A/B/C*, *135*, 103647.

Khaleel, M. H., AL RUKABIE, J. S., Al-Jiboori, M. H., & Al-Ramahy, Z. A. (2025). Relationships between daily solar irradiance and maximum temperature in Iraq. *Journal of Agrometeorology*, *27*(1), 67-72. https://doi.org/10.54386/jam.v27i1.2708

Lee, H., Calvin, K., Dasgupta, D., Krinner, G., Mukherji, A., Thorne, P., Trisos, C., Romero, J., Aldunce, P., & Barret, K. (2023). IPCC, 2023: Climate change 2023: Synthesis report, summary for policymakers. Contribution of working groups i, II and III to the sixth assessment report of the intergovernmental panel on climate change [core writing team, h. Lee and j. Romero (eds.)]. IPCC, Geneva, Switzerland.

Store, C. C. D. (2023). ERA5 hourly data on single levels from 1940 to present. *Copernicus Climate Change Service (C3S)*.

Tiku, T. W., Tarekegn, G. B., Sahlu, D., Tashebo, G. B., Enyew, F. B., Umer, Y., & Debele, S. E. (2025). Evaluating CMIP6 precipitation simulations across different rainfall regimes in the Amhara Region, Ethiopia. *Natural Hazards Research*, *5*(3), 689–704.

Wahab, B. I., Al-Tameemi, M. A., & Albaali, G. (2023). Analysis of a Dust Storm Profile: A Case Study in Iraq. *The Iraqi Geological Journal*, 301–308.